

HHS Public Access

Author manuscript

Proc IEEE Int Symp Biomed Imaging. Author manuscript; available in PMC 2019 November 22.

Published in final edited form as:

Proc IEEE Int Symp Biomed Imaging. 2018 April; 2018: 224–227. doi:10.1109/ISBI.2018.8363560.

IMPROVING TUMOR CO-SEGMENTATION ON PET-CT IMAGES WITH 3D CO-MATTING

Zisha Zhong^{*}, Yusung Kim[†], Leixin Zhou^{*}, Kristin Plichta[†], Bryan Allen[†], John Buatti[†], Xiaodong Wu^{*,†}

*Department of Electrical and Computer Engineering, University of Iowa, Iowa City, IA

†Department of Radiation Oncology, University of Iowa, Iowa City, IA

Abstract

Positron emission tomography and computed tomography (PET-CT) plays a critically important role in modern cancer therapy. In this paper, we focus on automated tumor delineation on PET-CT image pairs. Inspired by co-segmentation model, we develop a novel 3D image co-matting technique making use of the inner-modality information of PET and CT for matting. The obtained co-matting results are then incorporated in the graph-cut based PET-CT co-segmentation framework. Our comparative experiments on 32 PET-CT scan pairs of lung cancer patients demonstrate that the proposed 3D image co-matting technique can significantly improve the quality of cost images for the co-segmentation, resulting in highly accurate tumor segmentation on both PET and CT scan pairs.

Index Terms—

image segmentation; interactive segmentation; lung tumor segmentation; image matting; cosegmentation

1. INTRODUCTION

PET-CT has been widely used in modern cancer imaging. Accurate tumor delineation from PET and CT plays an important role in tumor staging, clinical management/decision making, treatment planning, and therapy response assessment. The PET-CT co-segmentation technique, which makes use of advantages of both modalities, has achieved impressive performance for tumor segmentation [1, 2].

In the past decades, extensive endeavors have been made on automated tumor definition from PET-CT scans. Recently, the co-segmentation technique for tumor delineation on both PET and CT images has been attracted great attentions [3, 4, 5, 6, 7]. In those works, tumor contours on PET and on CT are segmented simultaneously while admitting their possible differences. On the other hand, as demonstrated in those previous works, the design of cost functions in the framework of graph based co-segmentation is critical to achieve good segmentation performance. Consequently, the region/unary costs were usually designed carefully based on some sophisticated image priors (e.g., Gaussian mixture models [3, 4], shape prior [7], texture information [6], ...etc.) or clinical information from expertise [4, 5, 6, 7].

Recently, Zhong et al. [8] have introduced the 3D alpha matting technique to compute the region costs for graph-cut based PET-CT co-segmentation. The 3D alpha matting in [8] is conducted separatly on PET and on CT images, which may not make use of the modality-wise contextual information. In this paper, inspired by the co-segmentation model [4], we develop a novel 3D alpha matting technique for PET-CT co-segmentation. Specifically, the 3D alpha matting is jointly computed on both PET and CT images by "minimizing" the difference between their matte values. The resulting matte values are then used to design the region costs in the co-segmentation model [4]. Compared to previous PET-CT segmentation approaches, the proposed method is also completely image-derived with less relying on image and clinical priors. By integrating the proposed 3D alpha co-matting technique into the context-aware co-segmentation framework [4], the proposed PET-CT 3D co-matting method eases the design of cost functions for the graph-cut based segmentation, and significantly outperforms the PET-CT co-segmentation approach [4].

2. METHODOLOGY

Zhong et al. [8] have extended the 2D alpha matting [9] to 3D and propose to adopt the "matte" values to compute tumor object probability maps for the subsequent co-segmentation. In this work, inspired by the co-segmentation model, we further extend the 3D alpha matting to handle multi-modality image scans to simultaneously compute the matte values for voxels in different image modalities by considering the mutually interacting contextual information between the modalities.

The proposed PET-CT tumor segmentation method is semi-automated, and the general framework is mostly similar to that in [8], which mainly consists of three steps: (1) Active contour is adopted to generate larger seed regions from given initial seeds on PET and CT image pairs, respectively. (2) Based on the new seed regions, 3D image co-matting is jointly conducted on both PET and CT volumes to obtain the tumor object probability maps, which are further used for computing region/unary costs for the co-segmentation model [4]. This is the **main improvement** from that in [8]. The key contribution of this paper is to compute the region costs with the proposed 3D co-matting technique. (3) The PET-CT co-segmentation is formulated as a a Markov Random Field (MRF) optimization problem with label-consistency constraint, which penalizes the segmentation difference between the two image datasets. The optimization problem can be solved optimally by the well-known max-flow/min-cut algorithm to obtain the simultaneous tumor segmentation results [4].

Due to the space limit, we will mainly focus on the second step of the proposed method. The detailed description of Step (1) and (3) can be found in Ref. [8]. In the following, we first briefly review the 3D alpha matting technique [8], then introduce the proposed 3D alpha comatting algorithm in detail.

2.1. 3D alpha matting

Given a 3D image I with size of $H \times W \times D$, the 3D alpha matting [8] can be formulated as:

$$\alpha = \arg\min_{\alpha} \alpha^T L \alpha + \lambda (\alpha^T - b_S^T) D_S(\alpha - b_S), \tag{1}$$

where $\alpha \in \mathbb{R}^{N \times 1}$ is the alpha matte vector for all $N = W \times H \times D$ voxels, and $L \in \mathbb{R}^{N \times N}$ is a image-adaptive matting Laplacian matrix, λ is a coefficient, D_S is a diagonal matrix with an element 1 for each seed voxel and with an element 0 for each of the non-seed voxels, b_S is a vector indicating the alpha values for the seed voxels. Since (1) is a quadratic optimization problem, we can obtain the final global optimum solution by solving a sparse linear system [9].

By considering the neighborhood relationships among spatially in-slice adjacent voxels and those adjacent voxels between slices (e.g., $3 \times 3 \times 3$ neighborhood), the constructed matting Laplacian matrix L can better model tumor object structures, and consequently the probability maps (i.e. matting vector α) generated from alpha matting help produce better segmentation results. Zhong et al.[8] have applied the 3D alpha matting technique to generate the alpha matte map for each of the PET and CT datasets, separately, for the purpose of PET-CT co-segmentation of tumors. However, the two separately computed matte maps may not well make use of the contextual information of the other modality.

2.2. 3D alpha co-matting

In this subsection, we propose a novel 3D alpha co-matting method to compute two alpha matte maps for the PET and CT scans simultaneously. The mutual contextual information from both modalities is well integrated in the computation of alpha matting.

In the proposed method, we first generate a trimap using the user-given seeds in the same way as described in [8]. Based on the trimap, the 3D co-matting problem is formulated as optimizing the objective function $\mathcal{N}(\alpha, \beta)$, with:

$$J(\alpha,\beta) = \alpha^T L_1 \alpha + \lambda_1 \left(\alpha^T - b_S^T\right) D_S \left(\alpha - b_S\right) + \beta^T L_2 \beta + \lambda_2 \left(\beta^T - b_S^T\right) D_S \left(\beta - b_S\right) + \lambda_3 \left\|\alpha - \beta\right\|_2^2,$$

where α and β corresponds to the alpha matte maps for the input CT and PET images, respectively. The first two terms is the energy function for alpha matting on the CT images. The third and the fourth terms compose of the energy function for alpha matting on the PET image. The last term is to enforce the consistency between the alpha matte values of the corresponding voxels in PET and CT images. The alpha mattes on the input CT and PET images should be ideally as same as possible for the corresponding voxels. L_1 and L_2 are the matting Laplacian matrices on CT and PET images, respectively. λ_1 , λ_2 and λ_3 are regularization constants.

We solve this model iteratively using the alternative optimization, i.e., fix one variable, and solve another variable. For example, fix β , we can solve the α easily by

$$(L_1 + \lambda_1 D_S + \lambda_3 I)\alpha = \lambda_1 b_S + \lambda_3 \beta, \tag{2}$$

and similarly, the β can be updated by

$$(L_2 + \lambda_2 D_S + \lambda_3 I)\beta = \lambda_2 b_S + \lambda_3 \alpha. \tag{3}$$

The final solution is iteratively achieved until it converges. The initial α and β are computed by solely solving alpha matting problem for the CT and PET images, respectively (i.e., set λ_3 to zero). In practice, the convergence speed is very fast (less than 5 iterations in our experiments). The proposed method is summarized in Algorithm 1.

Algorithm 1 3-D Co-Matting algorithm.

Input: CT image \mathbf{X}_{CT} , PET image \mathbf{X}_{PET} , User-defined seeds \mathbf{b}_{S} ; size of neighborhood window r, number of maximum iterations T, converge precision ϵ ; parameters λ_1 , λ_2 , λ_3 .

Output: Alpha mattes α and β .

```
Compute the L_1 and L_2 as that in [8];
2:
                          Compute the a_0 and \beta_0 by (1);
3:
                          for t = 1, \dots, T do
4:
                                1) Set a_{old} = a_{t-1}
5:
                                2) Solve a_{\mathcal{L}} subproblem by Eqn. (2)
6:
                                3) Solve \beta_t subproblem by Eqn. (3)
                                if \|a_t - a_{t-1}\|_F \le \epsilon then
7:
8:
                                   break
9:
                                end if
10:
                          end for
```

Finally, two alpha matte maps for PET and CT with consistency constraints are obtained from the 3-D co-matting procedure. We then utilize the alpha mattes obtained from PET and CT images to compute the unary costs and give them as inputs to a graph cut based co-segmentation model [4] to obtain the final segmentation results.

3. EXPERIMENTS

3.1. Datasets

A total of 32 PET-CT scan pairs from different patients with primary non-small cell lung cancer were obtained. The image spacing varies from $0.78 \times 0.78 \times 2 mm^3$ to $1.27 \times 1.27 \times 3.4 mm^3$. The intra slice image size is 512×512 . The number of slices varies from 112 to 293. Two manual contours for each scan on both PET and CT images were provided by two physicians and we utilized the Simultaneous Truth And Performance Level Estimation (STAPLE) algorithm [10] to generate the reference standard for each scan of PET and CT.

3.2. Experiment Settings

All 32 PET-CT scans are separated disjoint as a training set (8 scans) and a testing set (24 scans) according to the similar strategy in [8]. All parameters are tuned on the training set. All reported results are from the testing set.

The same initialization procedure as in [8] is employed. A grid search strategy is used to tune the parameters. The parameters returning highest segmentation performance on training set are used to run the co-segmentation on the test set. In experiments, we select the λ_1 , λ_2 , and λ_3 from a specific range of [1, 10, 100, 1000, 10000]. Their final values are empirically set to all 1000, respectively. All other parameters are selected according to the similar strategy as those in [8].

The segmentation accuracy is measured by the Dice coefficient (DSC) as adopted in [8]. The higher the DSC is, the better volume overlap the two segmentations have. We conduct quantitative comparisons to the matting-based PET-CT co-segmentation methods of Song *et al.*'s [4] and Zhong *et al.*'s [8].

3.3. Results and analysis

Table 1 reports the mean DSCs and standard deviations of the evaluated methods on the test scans. From these results, we have the following observations. First, compared to Song's co-segmentation method, our 3D matting based methods can achieve much better performance with higher DSCs (on average, 10% or more improvements) with significant confidences (if p-values is thresholded by 0.005). Second, compared to our previous method studied in [8], the proposed co-matting based segmentation method achieves a comparable or even better average performance, which validates the efficiency of the proposed 3D co-matting procedure. This is mainly owing to that our co-matting based co-segmentation method considers multi-level intra-modality information interaction. Fig. 1 shows the segmentation results of the compared methods on two PET-CT scans. From those figures, we can see our matting or co-matting based methods are able to locate tumor boundaries more accurately in these scans.

Fig. 2 shows the convergence curves when solving the problem of (2) with different regularization parameters. First we select the values of λ_1 and λ_2 as suggested in [8], then draw the convergence curves with variable λ_3 s. In our experiments, we found the proposed approach achieves better average performance with a relatively large value of λ_3 . Note that although our method can achieve better performance over the previous methods on most scans, the hyperparameter selection is still relatively difficult given the limited number of training scans, especially when there are much different volume sizes of tumors in the data sets. The parameters selected on those fixed training scans might not perform well on other scans. How to automatically, adaptively and effectively determine these hyperparameters according to input images is still actively challenging in this field.

On the other hand, in our experiments, we can also observe that, on PET images with relatively small tumors, our results seems to be not significant compared to others. And the average performance on these scans is overal inferior to those with big tumors. The main reason lies in that when the tumor is too small, it is commonly difficult to determine the tumor boundary accurately, and consequently small changes on segmentation results may lead to significantly corrupt performances evaluated by DSC. In the future, we will resort to more intelligent solutions on these challenges for tumor segmentation task on PET-CT image pairs, e.g. the recently-boomed deep learning technique [11].

4. CONCLUSION

In this paper, we have developed a 3D co-matting approach to generate high-quality region cost for both PET and CT images by considering the inter-modality context information during the matting process. When integrated with the powerful graph-cut based PET-CT co-segmentation model, our proposed method is able to detect highly accurate tumor boundaries from both PET and CT. The experimental results on 32 non-small cell lung cancer PET-CT image scan pairs demonstrated the effectiveness of the proposed method.

Acknowledgments

This work was supported in part by the National Science Foundation (NSF) under Grant CCF-1733742, and in part by the the National Institutes of Health (NIH) under Grants R01-EB004640 and 1R21CA209874.

5. REFERENCES

- [1]. Bagci Ulas, Udupa Jayaram K., Mendhiratta Neil, Foster Brent, Xu Ziyue, Yao Jianhua, Chen Xinjian, and Mollura Daniel J., "Joint segmentation of anatomical and functional images: Applications in quantification of lesions from PET, PET-CT, MRI-PET, and MRI-PET-CT images," Medical Image Analysis, vol. 17, no. 8, pp. 929–945, 12 2013. [PubMed: 23837967]
- [2]. Foster Brent, Bagci Ulas, Mansoor Awais, Xu Ziyue, and Mollura Daniel J., "A Review on Segmentation of Positron Emission Tomography Images," Computers in biology and medicine, vol. 0, pp. 76–96, 7 2014.
- [3]. Han Dongfeng, Bayouth John, Song Qi, Taurani Aakant, Sonka Milan, Buatti John, and Wu Xiaodong, "Globally Optimal Tumor Segmentation in PET-CT Images: A Graph-Based Co-Segmentation Method," Information processing in medical imaging: proceedings of the ... conference, vol. 22, pp. 245–256, 2011. [PubMed: 21761661]
- [4]. Song Q, Bai J, Han D, Bhatia S, Sun W, Rockey W, Bayouth JE, Buatti JM, and Wu X, "Optimal Co-Segmentation of Tumor in PET-CT Images With Context Information," IEEE Transactions on Medical Imaging, vol. 32, no. 9, pp. 1685–1697, 9 2013. [PubMed: 23693127]
- [5]. Li H, Bai J, Abu Hejle T, Wu X, Bhatia S, and Kim Y, "Automated Cosegmentation of Tumor Volume and Metabolic Activity Using PET-CT in Non-Small Cell Lung Cancer (NSCLC)," International Journal of Radiation Oncology * Biology * Physics, vol. 87, no. 2, pp. S528, 10 2013.
- [6]. Lartizien C, Rogez M, Niaf E, and Ricard F, "Computer-Aided Staging of Lymphoma Patients With FDG PET/CT Imaging Based on Textural Information," IEEE Journal of Biomedical and Health Informatics, vol. 18, no. 3, pp. 946–955, 5 2014. [PubMed: 24081876]
- [7]. Ju W, Xiang D, Zhang B, Wang L, Kopriva I, and Chen X, "Random Walk and Graph Cut for Co-Segmentation of Lung Tumor on PET-CT Images," IEEE Transactions on Image Processing, vol. 24, no. 12, pp. 5854–5867, 12 2015. [PubMed: 26462198]
- [8]. Zhong Zisha, Kim Yusung, Buatti John, and Wu Xiaodong, "3d Alpha Matting Based Cosegmentation of Tumors on PET-CT Images," in Molecular Imaging, Reconstruction and Analysis of Moving Body Organs, and Stroke Imaging and Treatment, Lecture Notes in Computer Science, pp. 31–42. Springer, Cham, 9 2017.
- [9]. Levin A, Lischinski D, and Weiss Y, "A Closed-Form Solution to Natural Image Matting," IEEE Transactions on Pattern Analysis and Machine Intelligence, vol. 30, no. 2, pp. 228–242, 2 2008. [PubMed: 18084055]
- [10]. Warfield SK, Zou KH, and Wells WM, "Simultaneous truth and performance level estimation (STAPLE): an algorithm for the validation of image segmentation," IEEE Transactions on Medical Imaging, vol. 23, no. 7, pp. 903–921, 7 2004. [PubMed: 15250643]
- [11]. Shen Dinggang, Wu Guorong, and Suk Heung-Il, "Deep Learning in Medical Image Analysis," Annual review of biomedical engineering, vol. 19, pp. 221–248, 6 2017.

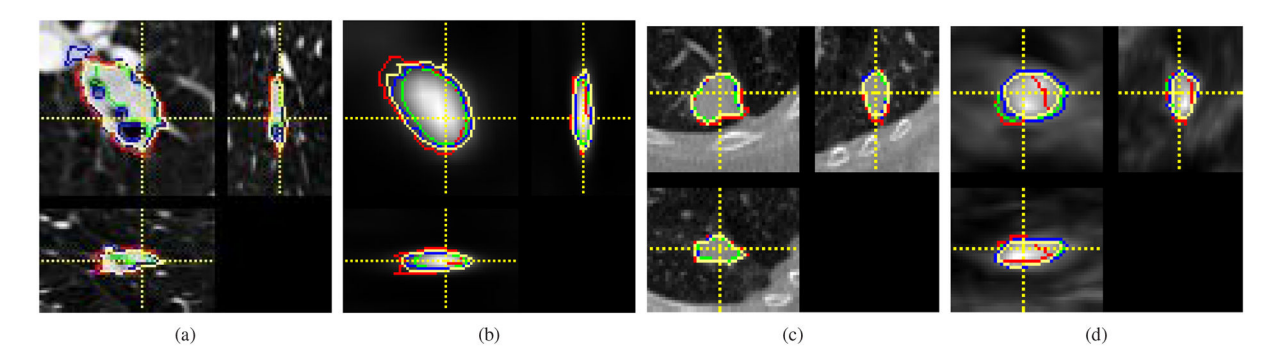
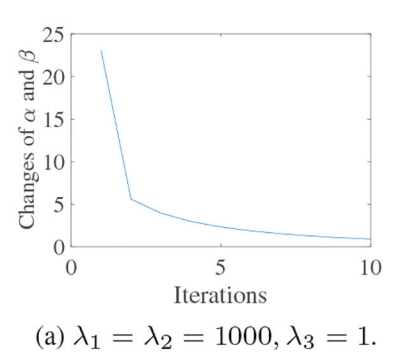


Fig. 1.
Segmentation results of compared methods on two PET-CT scans: No. 0002118 and No. 002133. Red: ground truth, Green: Song's method [4], Blue: Zhong's method [8], Yellow: Proposed method.



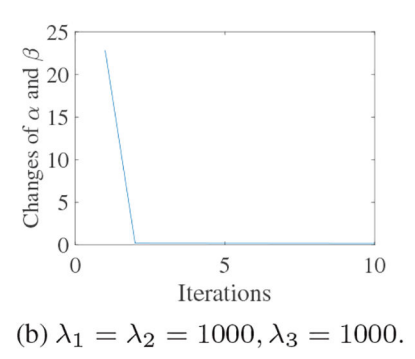


Fig. 2. Convergence curves for different λ_3 s.

Table 1.Average DSC's and standard deviations of three compared methods.

Methods	Modalities	DSC	p-values
Song et al. [4]	CT	0.620 ± 0.229	
	PET	0.668 ± 0.134	
Zhong et al. [8]	CT	0.752 ± 0.102	0.0038
	PET	0.762 ± 0.079	0.0005
Proposed	CT	0.778 ± 0.109	0.0009
	PET	0.811 ± 0.064	0.0001